02

Photocatalytic properties of MgO−ZnO composites modified with Cu and Mn ions

© D.A. Gavrilova[1,2], M.A. Gavrilova[1], S.K. Evstropiev[1,2,3]

[1] St. Petersburg State Institute of Technology, St. Petersburg, Russia
[2] Vavilov State Optical Institute, St. Petersburg, Russi
[3] ITMO University, St. Petersburg, Russia

e-mail: amonobel@yandex.ru

Received April 30, 2025
Revised November 17, 2025
Accepted November 24, 2025

In this work, composites of the ZnO−MgO system modified with Cu and Mn ions were synthesized using the polymer sol-gel method. Their crystal structure, morphology, adsorption and photocatalytic properties, as well as the ability to photogenerate singlet oxygen were studied. The structure and properties of the materials were studied using X-ray diffraction, scanning electron microscopy and energy dispersive X-ray analysis, optical and luminescence spectroscopy. The obtained powder composites are characterized by a highly porous structure and consist of ZnO and MgO nanocrystals less than 20 nm in size. It was found that modifying ions Cu^{2+} and Mn^{2+} are introduced into the crystal lattices of ZnO and MgO during the synthesis and change their parameters. It was shown that ZnO−MgO composites modified with Cu and Mn ions have the ability to photogenerate chemically active singlet oxygen under the action of visible radiation ($\lambda = 405$ nm). The composites demonstrate high rates of adsorption and photocatalytic decomposition of the Chicago Sky Blue diazo dye in aqueous solutions under the action of radiation with a wavelength of 395 nm. The dye adsorption kinetics is described by a pseudo-second-order kinetic equation. The composites demonstrate a high rate of photocatalytic dye degradation, described by a pseudo-first-order kinetic equation.

Keywords: photocatalysis, MgO and ZnO nanocrystals, singlet oxygen.

DOI: 10.61011/0000000000

Introduction

Environmental issues are driving the development of photocatalytic materials and processes. Many semiconductor oxides (TiO_2, ZnO, SnO_2, and others) exhibit high photocatalytic properties and antibacterial activity, while possessing chemical resistance and heat resistance [1–5]. Numerous studies have established that the main mechanism providing high photocatalytic properties and antibacterial activity of these materials is their generation of various reactive oxygen species (ROS) [6–10].

It is known that the morphology of materials has a significant effect on their adsorption and photocatalytic properties, which determines the effectiveness of removing organic pollutants, purifying and disinfecting air and aquatic media [11]. The adsorption of organic compounds from the gas or liquid phases onto the surface of the photocatalyst plays an important role in the process of their photocatalytic decomposition. Adsorption processes have been the subject of numerous studies devoted to photocatalytic processes [2,12–15]. It has been found that adsorption is particularly active on the surface of materials with a high specific surface area, which increases their photocatalytic activity. The processes of adsorption and photocatalysis using various porous materials characterized by a high specific surface area are described in Ref. [2,12–14,16,17].

Many studies ([11,18–21]) have shown that multicomponent semiconductor composites exhibit higher photocatalytic and bactericidal properties compared to their single-component counterparts. One of the promising multicomponent photocatalytic materials are composites of the ZnO−MgO system [22,23].

A strong influence on the structure of ZnO crystals and their properties is observed when they are modified by relatively small amounts of transition metal oxides (Sn [18,24], Mn [11,25,26], Fe [21], Cu [13,25], Ag [27]). It was shown in Ref. [25] that modification of ZnO nanoparticles with Ag, Cu, and Mn ions increases their photocatalytic activity under the influence of visible-range radiation. Modification of the composites of the ZnO−MgO system with small amounts of Ag significantly enhances their ability to photogenerate ROS and provides high antibacterial activity [27].

It is known that ions Mn^{2+} and Cu^{2+} are capable of replacing zinc ions in ZnO crystals [7,8,20,28–32]. According to data from Ref. [1], modification of ZnO crystals with manganese or copper ions provided a significant increase in the photocatalytic activity of ZnO when exposed to visible light. It is known that modification of ZnO particles by manganese ions can increase their specific surface area [28], change the band gap of the material, and affect the formation of structural defects in it [28,29]. In particular, modification of ZnO

crystals by manganese ions can lead to a decrease in the concentration of zinc ion vacancies in the crystal lattice and increase the concentration of oxygen vacancies.

It should be noted that the structure and properties of oxide composite materials based on ZnO are strongly influenced by the content of the modifying component. Thus, it was shown in Ref. [28] that when the solubility limit of ions Mn^{2+} was exceeded in the ZnO crystal lattice, the formation and aggregation of crystals $ZnMnO_3$ and an increase in the structural defects of composite materials were observed. This phenomenon was observed in Ref. [28] in composites containing ≥ 15 mass.% MnO.

It was shown in Ref. [33] that the modifying additives Mn and Cu have a noticeable effect on the photoluminescence spectra of ZnO nanoparticles obtained from solutions and their photocatalytic activity under the influence of UV radiation. At the same time, the observed change in the properties of ZnO nanoparticles depends both on the characteristics of their synthesis and on the concentration of the introduced modifying ions. Based on the experimental results obtained, it was concluded that with an increase in the content of modifying additives Cu and Mn, the photocatalytic activity of ZnO nanoparticles decreases slightly when exposed to UV radiation.

Based on a comparison of the data from Ref. jcite1,33 it can be concluded that the effect of the modifying additives Mn and Cu on the photocatalytic activity of ZnO strongly depends on the wavelength of the exciting radiation. An increase in the photocatalytic activity of zinc oxide nanoparticles with the introduction of these modifying ions is manifested when using radiation with photon energy, less than the band gap of ZnO.

The purpose of this work is to study the effect of Mn and Cu additives on the structural, adsorption, and photocatalytic properties of ZnO−MgO system materials.

Materials and methods

The polymer sol-gel method was used for the synthesis of composites. Aqueous solutions of $Zn(NO_3)_2$, $Mg(NO_3)_2$, $Cu(NO_3)_2$, $Mn(NO_3)_2$ (all C.P.) were mixed with a solution of polyvinylpyrrolidone (PVP, AR, $M_w = 25000-35000$). The resulting composite solution was stirred at room temperature for 1 h. Next, the solution was dried at 70 °C for 24 hours, after which the resulting gels were subjected to heat treatment at 550 °C for 2 hours in an air atmosphere. This heat treatment mode ensures the complete decomposition of metal nitrates and PVP and the removal of gaseous products [30].

The morphology and elemental composition of the obtained oxide powders were studied by scanning electron microscopy using a TescanVega 3 SBH microscope equipped with an Oxford INCA X-act X-ray energy-dispersive X-ray analysis device (EDX). The chemical composition of composites determined by the EDX method is shown in

Table 1. Analytical chemical composition of materials

Sample	Analytical chemical composition of powders, mol.%			
	ZnO	MgO	CuO	MnO
1	39.26	60.74	–	–
2	38.37	60.35	1.28	–
3	35.31	64.11	–	0.59
4	36.73	62.76	0.28	0.24
5	32.13	67.41	0.18	0.28

Table 1. The error of the spectral equipment used is error shown in Table 2.

The crystal structure of the materials was studied by X-ray phase analysis with a Rigaku Ultima IV diffractometer with the following parameters: radiation CuK_α ($\lambda = 1.54056$ Å), 40 kV, 30 mA, scanning speed 2°/min. The Scherrer formula was used to estimate the sizes of crystallites in the materials:

$$d = \frac{K\lambda}{\beta \cos\theta}, \quad (1)$$

where d is the average crystallite size, K is the dimensionless particle shape factor (for spherical particles $K = 0.9$), λ is the radiation wavelength (Cu$K_\alpha = 1.5418$ Å), β is the peak width at half peak height (in radians), θ is the diffraction angle.

It is known from Ref. [31] that chemically active singlet oxygen exhibits characteristic phosphorescence in the near-IR spectral range ($\lambda_{max} = 1270$ nm). In the present work, the luminescent method described in Ref. [31] was used to study the photogeneration of singlet oxygen by the obtained composite materials under the influence of visible-range radiation using an HPR40E ($\lambda = 405$ nm) LED.

Aqueous solutions of Chicago Sky Blue (CSB) diazo dye (Sigma Aldrich, St. Louis, MO, USA), which was used as a model organic contamination, was used to evaluate the photocatalytic activity of the composites synthesized by us. This dye was previously used in studies of the photocatalytic properties of various materials [34,35]. The photocatalytic properties of the composites were studied by adding 0.005 g of composite to 3 ml of a 0.01 g/l dye solution. A cuvette with a dye solution and a composite additive was placed to a light source using a narrow-band LED with a wavelength of 395 nm. The dye concentration in the solution was determined by the spectrophotometric method.

Results and discussion

X-ray phase analysis studies have shown the presence of hexagonal ZnO crystals in all composites (Fig. 1). The ratio of the intensities of the various peaks of zinc oxide crystals in the diffraction patterns is close to the standard (ICSD 067848). Calculations performed using the Scherrer formula showed that the average size of ZnO crystals in all composites does not exceed 20 nm.

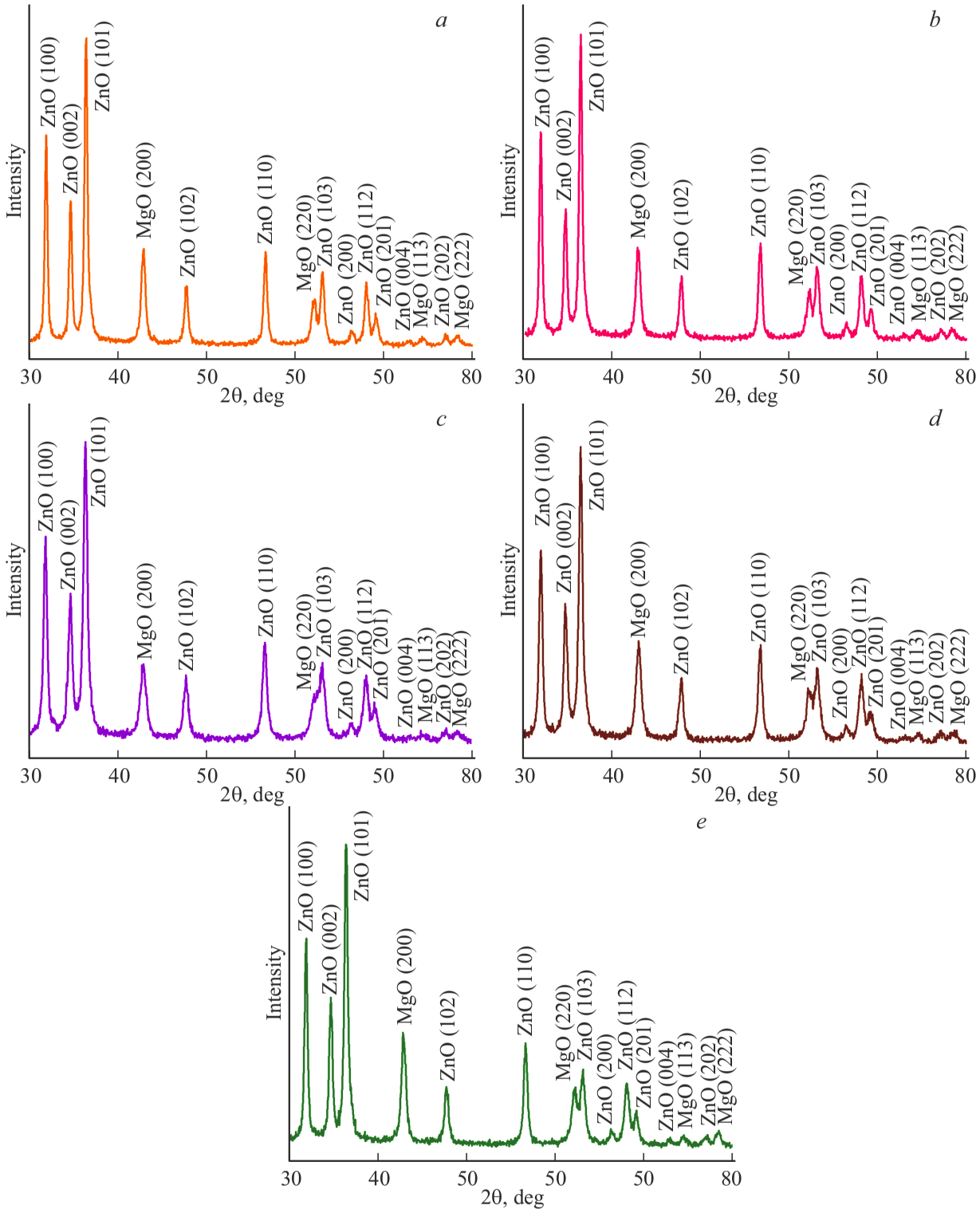


Figure 1. X-ray patterns of composites **1**–**5** (*a*–*e*, respectively).

Zn^{2+}ions are located in hexagonal ZnO crystals in tetrahedral coordination and the ion radius of Zn^{2+}(IV) is 0.6 Å [36]. Mg^{2+}(IV), Mn^{2+}(IV), and Cu^{2+}(IV) ions have ionic radii 0.57, 0.66, 0.57 Å, respectively, [37] and can replace zinc ions in ZnO crystals [28,38–40].

Table 3 shows the parameters of the unit cells of ZnO crystals in various materials. A comparison with the literature data shows that in zinc oxide crystals in synthesized composites, there is a slight decrease in the values of c, c/a, and V, which may be due to deformation

Table 2. Metrological characteristics of spectral equipment

Analysis	Instrument	Sensitivity	Error	
			Relative in range	%
PCMA	Oxford INCA X-act	0.01 mass.%	0.1−1.5 mass.%	35
			1.5−10 mass.%	30
			10−20 mass.%	10
			20−100 mass.%	5
Photoluminescent spectroscopy	Perkin Elmer LS-50B	signal to noise ratio 500:1	absolute for wavelength ±1 nm	
UV visible Spectroscopy	Perkin Elmer Lambda 650 UV/VIS	for optical Density 0.001	absolute for optical density ±0.003	

Table 3. Parameters of elementary cells of ZnO crystals in various materials

Sample	a, Å	c, Å	V, Å^3	c/a	Source
1	3.2538	5.1955	47.637	1.5968	This study
2	3.2528	5.1914	47.568	1.5960	This study
3	3.2540	5.1892	47.585	1.5947	This study
4	3.2533	5.1898	47.569	1.5952	This study
5	3.2527	5.1908	47.561	1.5958	This study
ZnO	3.2535	5.2151	47.81	–	ICSD 067848
ZnO	3.2501	5.2071	47.63	1.6021	[40]
ZnO	3.2487	5.1989	47.52	1.6003	[37]
ZnO	3.251	5.210	47.667	1.601	[23]
$Zn_{0.99}Mn_{0.01}O$	3.2500	5.2030	47.59	1.6009	[37]
$Zn_{0.95}Mn_{0.05}O$	3.2493	5.2023	47.57	1.6010	[37]
$Zn_{0.99}Mg_{0.01}O$	3.2518	5.2102	47.722	1.602	[41]
$Zn_{0.98}Mg_{0.02}O$	3.2518	5.2102	47.722	1.602	[41]
$Zn_{0.95}Mg_{0.05}O$	3.2522	5.2101	47.734	1.602	[41]
ZnO	3.2764	5.1874	–	1.5832	[39]
$Zn_{0.996}Mg_{0.004}O$	3.2795	5.1906	–	1.5827	[39]
$Zn_{0.992}Mg_{0.008}O$	3.2827	5.1907	–	1.5812	[39]
$Zn_{0.988}Mg_{0.012}O$	3.2922	5.1997	–	1.5794	[39]
$Zn_{0.984}Mg_{0.016}O$	3.3049	5.2122	–	1.5771	[39]
$Zn_{0.980}Mg_{0.020}O$	3.3081	5.2167	–	1.5770	[39]
$Cu_{0.0417}Zn_{0.9583}O$	3.272	5.284	–	1.5967	[36]
$Cu_{0.0278}Zn_{0.9722}O$	3.249	5.205	–	1.6020	[36]

of the ZnO crystal lattice by modifying ions embedded in it. A decrease in c/a values in modified ZnO crystals was observed earlier in Ref. [13,40,41].

Small peaks of cubic MgO crystals (ICSD 067848) are also observed on diffraction patterns. Mg^{2+} ions are found in cubic MgO crystals in octahedral coordination and the ion radius Mg^{2+}(VI) is 0.72 Å [37]. The ion radii of Zn^{2+}(VI), Mn^{2+}(VI), and Cu^{2+}(VI) are 0.74, 0.83, and 0.73 Å respectively [37], and these ions can replace Mg^{2+} in the structure of cubic MgO crystals. The size of MgO crystallites ranges from 9 to 14 nm.

Data on the position of peaks of MgO crystals on diffraction patterns of composites and calculated parameters of the unit cells of these crystals are listed in Table 4. It can be seen from the above data that the peaks on the diffraction patterns are shifted towards lower values of 2θ compared to the standard values (ICSD code 166273). This suggests that in the structure of MgO crystals, some of the magnesium ions could be replaced by larger ions (Zn^{2+}, Mn^{2+}, Cu^{2+}) and the unit cell in these crystals increased slightly in size. The absence of peaks of any copper and manganese compounds in the diffraction patterns (Fig. 1) further confirms this assumption. Figure 2 shows a diagram illustrating the effect of Mn^{2+} ion incorporation on the MgO crystal lattice.

Figure 3 demonstrates electron microscopic images of composites **1** (*a*), **2** (*b*) and **3** (*c*). It can be seen from the figure that all composites have a developed sponge-like structure. The formation of a similar structure in materials ZnO and ZnO−MgO obtained by polymer sol-gel synthesis

was explained in Ref. [2,22] by the strong release of gaseous products during the decomposition of metal nitrates and PVP during heat treatment of polymer gels during the synthesis of oxide materials. This structure of composite-sensures effective contact with the environment, which is important when usingthese materials in the processes of adsorption of organic compounds and theirphotocatalytic decomposition.

Figure 4 shows the phosphorescence spectra of composites in the near-infrared region of the spectrum when they are excited by radiation in the visible range ($\lambda = 405$ nm). The phosphorescence band characteristic of singlet oxygen with a maximum of $\lambda_{max} = 1270$ nm associated with the electronic transition $1\Delta_g - 3\Sigma_g$ is observed in the above spectra [31]. It should be noted that this phosphorescence is observed when composites are excited by blue light ($\lambda_{ex} = 405$ nm) with a photon energy of 3.06 eV, which is significantly less than the band gap of ZnO (3.37 eV) and MgO (7.8 eV). This phenomenon may be related to the influence of structural defects, which are often present in dispersed materials and play an important role in ROS generation and photocatalytic processes [16,31,42].

To study the adsorption properties of composites, their 0.01 g samples were placed in a cuvette containing 3 ml of a solution (0.01 g/l) of CSB dye. Figure 5 shows kinetic dependences of the adsorption of CSB dye from aqueous solutions on the surface of composites. All synthesized powders show high adsorption activity and after 30 min from the beginning of the experiment, only −20 % of the dye molecules remain in the solution. The difference in the rate of dye adsorption by different composites is small. Thus, the chemical composition within the selected limits has practically no effect on the adsorption kinetics, and adsorption is mainly determined by the close morphology of the obtained composites.

The Lagergren model and the pseudo-first order kinetic equation are often used to describe the kinetics of adsorption on the surface of photocatalytic materials:

$$\frac{dq_t}{dt} = k(q_e - q_t), \qquad (2)$$

where q_t (mg/g) is the amount of dye adsorbed by 1g of the sorbent during t; q_e (mg/g) is the equilibrium adsorption capacity of the sorbent; k (min^{-1}) is the rate constant of adsorption of the pseudo-first order; t is the duration of adsorption (min).

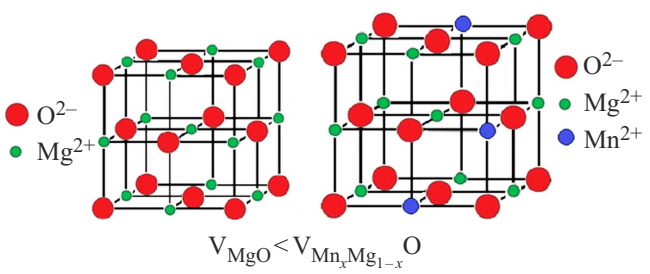


Figure 2. Illustrative diagram of the expansion of the unit cell of MgO crystals when ions Mn^{2+} are introduced into them.

Table 4. Position of the most intense peaks of MgO crystals on diffractograms of composites

Sample	(*hkl*)				
	(111)	(200)	(220)	(311)	(222)
MgO (ICSD 166273)	37.04	43.04	62.49	74.93	78.89
1	36.77	42.71	61.99	74.29	78.21
2	36.80	42.75	62.05	74.34	78.28
3	36.83	42.78	62.11	74.44	78.36
4	36.78	42.73	62.02	74.34	78.25
5	36.80	42.76	62.06	74.38	78.30
R, %	2.8	2.6	3.9	3.2	3.4

Fig. 5, *b* shows the dependences $-\ln(q_e - q_t) = f(t)$, obtained on the basis of experimental data on dye adsorption on the surface of composites. The data shown in Fig. 5, *b* shows that the equation (2) satisfactorily describes ($R_2 > 0.9$) the kinetics of CSB dye adsorption on the surface of all composites. This fact is consistent with the previously published results [12] that the kinetics of CSB dye adsorption on the surface of the ZnO–MgO composite corresponds well to the kinetic equation of the pseudo-first order.

Numerous experimental data from [12,42,44,45] show that the kinetic model of pseudo-second-order adsorption is also often used and more accurately describes the kinetics of adsorption on the surface of various materials. In the integral form, the equation of the kinetics of pseudo-second-order adsorption can be written as the equation [12,44]

$$\frac{t}{q_t} = \frac{1}{k_2 q_e^2} + \frac{t}{q_e}, \qquad (3)$$

where k_2 is the pseudo-second order adsorption rate constant, q_e is the maximum equilibrium adsorption capacity of the photocatalyst (mg/g), q_t is the content of the adsorbed dye on the surface of the photocatalyst at time t (mg/g). Fig. 5, *c* demonstrates the dependences $t/q_t = f(t)$ for dye adsorption on the surface of composites. It can be seen that the kinetics of dye adsorption on the surface of all composites is well described ($R^2 > 0.9$) by equation (3). A comparison of the data presented in Fig. 5, *b, c* shows that the pseudo-second order equation (3) describes the kinetics of dye adsorption better (R^2 is significantly greater) than the pseudo-first order equation (2).

Fig. 6, *a* demonstrates the kinetic dependences of the discoloration of dye solutions under the action of radiation with a wavelength of 395 nm in the presence of various composites. It can be seen fromthe figure that in the absence of composite additives, photolysis of the dye in solution proceeds slowly (Fig. 6, *a*, curve *1*). Composite additives significantly accelerate the discoloration of solutions (Fig. 6, *a*, curves *2–6*), while changes in

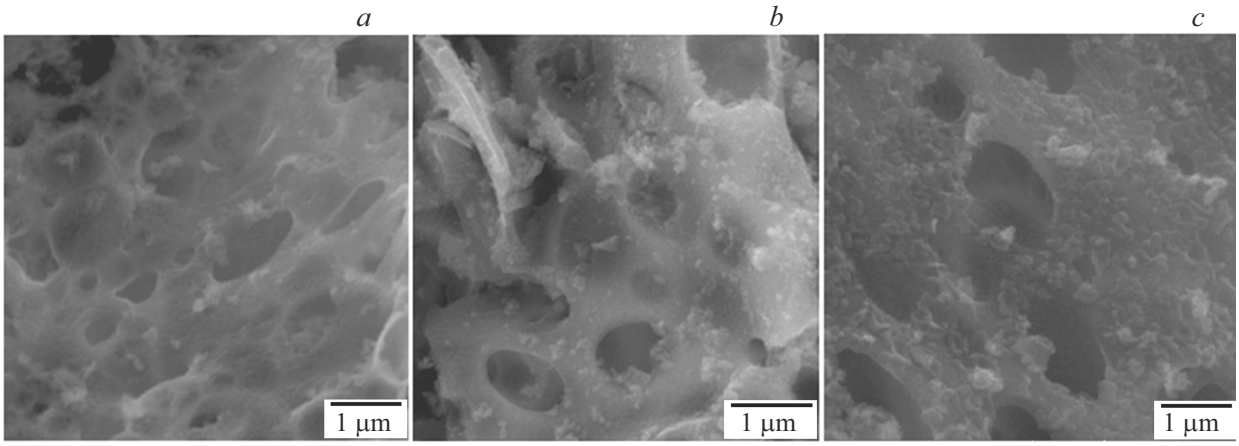


Figure 3. Electron microscopic images of composites **1**–**3** (*a*–*c*, respectively).

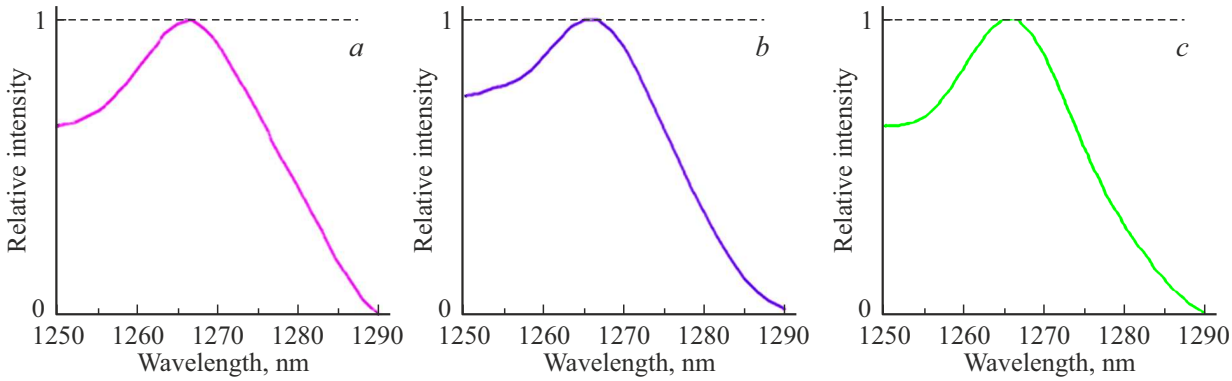


Figure 4. Phosphorescence spectra of composites **1** (*a*), **3** (*b*), **5** (*c*) in the near-IR region of the spectrum. The excitation wavelength is $\lambda_{ex} = 405$ nm.

the chemical composition of composites significantly affect the kinetics of photocatalytic decomposition of the dye. Figures 5, *a* and 6, *a* clearly show that in the case of adsorption, there is practically no difference in the kinetic curves C/C_0 of various composites (Fig. 5, *a*), while as with light irradiation, this difference is significant (Fig. 6, *a*), which indicates a difference in the photocatalytic properties of composites. Also, the photocatalytic dependences shown in Fig. 6, *b* are well ($R^2 > 0.95$) described by the kinetic equation of the pseudo-first order reaction.

Thus, the addition of a composite **1** to the dye solution, which does not contain modifying copper and manganese ions, significantly increases the rate of photoregradation of the dye and after photoregradation of the solution for 30 min, more than 40 % of CSB molecules undergo decomposition.

The use of composites **2**–**5** having a chemical composition similar to the composite **1**, but containing modifying manganese and copper ions, provides a significant increase in the rate of photocatalytic decomposition of CSB dye. The use of these composites ensures rapid photocatalytic decomposition of the dye in solution, and −80 % of CSB molecules are removed from the solution during a photo-treatment duration of 30 min. Also, a noticeable effect on the photocatalytic properties of ZnO particles by modification with copper and manganese ions was shown earlier in Ref. [25]. It should be noted that the rate of photocatalytic decomposition of CSB dye when using the composites synthesized in this work significantly exceeds the rate of decomposition of this dye, which was observed when using a photocatalyst of the ZnO–MgO system in Ref. [12].

One of the possible mechanisms of the observed high photocatalytic activity of Mn- and Cu-containing composites is an increase in light absorption at the wavelength of exciting radiation (395 nm) when these components are introduced into composite materials. For instance, an increase in light absorption at this wavelength was observed in Ref. jcite29, when ZnO was modified with manganese ions.

To describe the kinetics of photocatalytic decomposition of organic compounds in solutions, a pseudo-first-order kinetic equation is often used, which can be written as [12,46]

$$C/C_0 = e^{-kt}, \qquad (4)$$

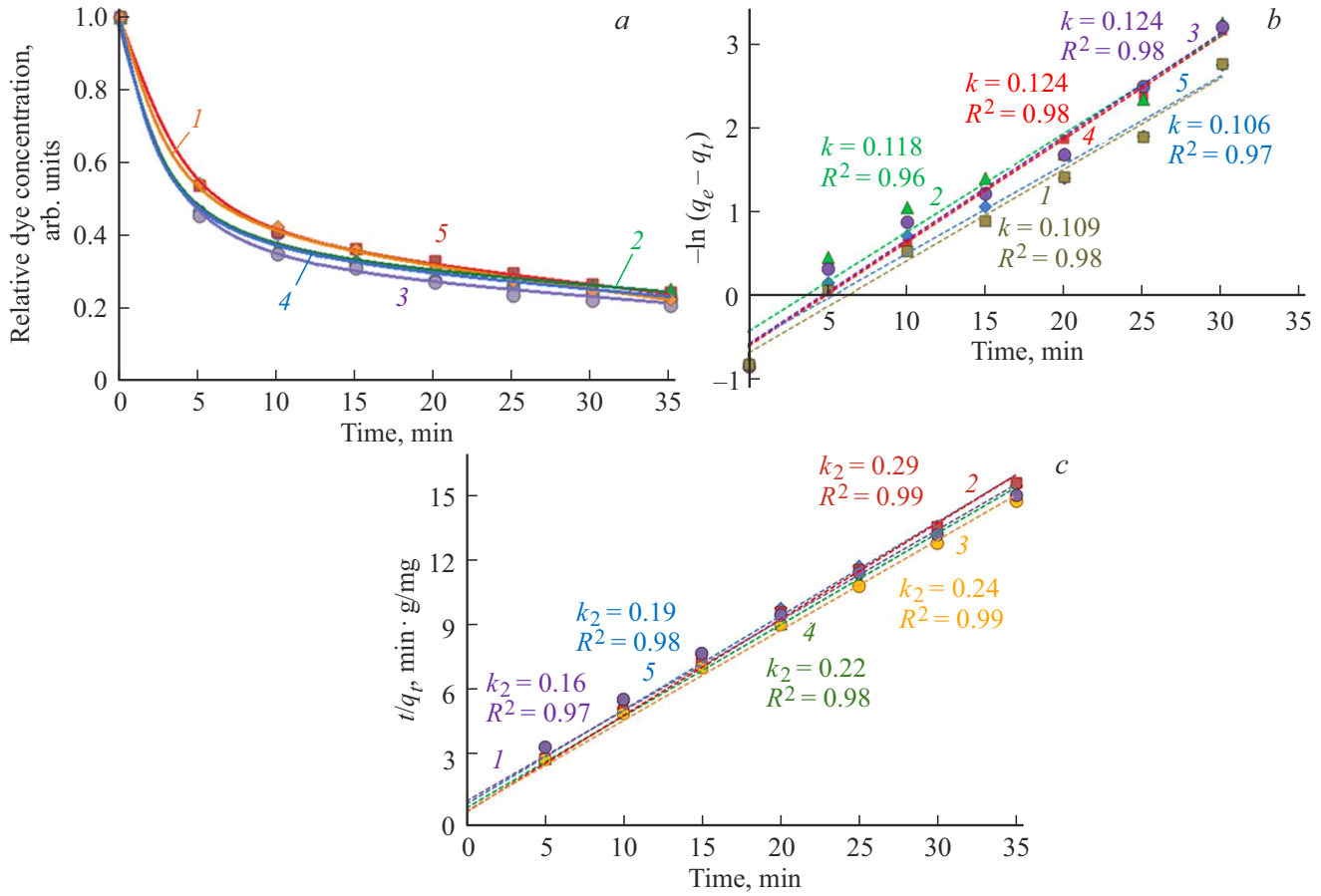


Figure 5. (*a*) Kinetic dependences of CSB dye adsorption on the surface of composites **1**–**5** (*1*–*5*, respectively); (*b*) dependencies $-\ln(q_e - q_t) = f(t)$ for CSB dye adsorption; (*c*) dependencies $t/q_t = f(t)$ for CSB dye adsorption. The samples are **1**–**5** (*1*–*5* respectively).

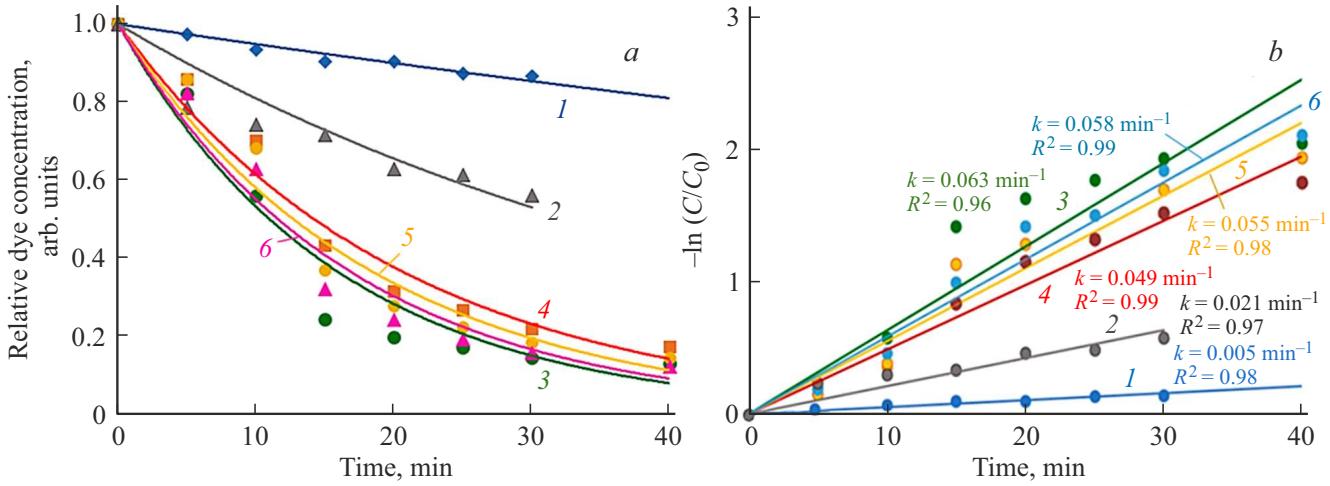


Figure 6. (*a*) Kinetic dependences of the discoloration of CSB dye solutions under the action of wavelength radiation ($\lambda_{max} = 395$ nm) in the presence of additives of various composites. Discoloration of dye solutions: without additives of composites (*1*); with additives of composites: **1** (*2*), **2** (*3*), **3** (*4*), **5** (*5*), **4** (*6*). (*b*) Dependencies $-\ln(C/C_0) = f(t)$, calculated based on experimental data. Samples: without additives of composites (*1*); with additives of composites: **1** (*2*), **2** (*3*), **3** (*4*), **5** (*5*), **4** (*6*).

where C_0 and C are the initial and current dye concentrations (mmol), t is the duration of irradiation (min), k is the rate constant of photocatalytic decomposition of the dye (min^{-1}).

Fig. 6, *b* shows the $-\ln(C/C_0) = f(t)$ dependencies obtained based on the data shown in Fig. 6, *a*. It can be seen from Fig. 6, *b* that all dependencies are linear ($R^2 \geq 0.96$). It should be noted that the values of the rate constants of photocatalytic decomposition of CSB dye obtained using composites **2÷5** containing modifying manganese and/or copper ions reach $0.063\,\text{min}^{-1}$ and significantly exceed the values of k observed using the composite **1**. Based on the data obtained, it can be concluded that modification of the MgO−ZnO system composites with small amounts of manganese and copper ions can significantly increase their photocatalytic activity when exposed to visible range radiation.

Conclusion

In the process of polymer sol-gel synthesis of composites of the MgO−ZnO system, modifying copper and manganese ions are introduced into the crystal lattices of ZnO and MgO, which leads to their deformation. The synthesized composites are characterized by a porous structure and the ability to photogenerate chemically active singlet oxygen under the influence of radiation in the visible spectral range ($\lambda = 405\,\text{nm}$).

The synthesized composites demonstrate a high rate of adsorption from aqueous solutions of CSB diaz dye. The kinetics of the adsorption process is well described by a pseudo-second-order kinetic equation.

The kinetics of photocatalytic decomposition of the CSBl diaz dye in the presence of composites under the action of radiation with a wavelength of $\lambda = 395\,\text{nm}$ is described by a kinetic equation of the pseudo-first order. Additives of MgO−ZnO composites modified with copper and manganese ions ensure a high rate of photocatalytic decomposition of the dye (decomposition rate constant $k = 0.049{-}0.063\,\text{min}^{-1}$).

References

[1] E.S. Araújo, M.F.G. Pereira, G.M.G. da Silva, G.F. Tavares, C.Y.B. Oliveira, P.M. Faia. Toxics, **11**, 658 (2023). DOI: 10.3390/toxics11080658

[2] M.A. Gavrilova, D.A. Gavrilova, S.K. Evstropiev, A.A. Shelemanov, I.V. Bagrov. Ceramics, **6** (3), 1667–1681 (2023). DOI: 10.3390/ceramics6030103K

[3] E.A. Kozlova, V.N. Parmon. Uspekhi khimii, **86** (9), 870–906 (2017) (in Russian). DOI: 10.1070/RCR4739

[4] Samriti, R. Tyagi, O. Ruzimuradov, J. Prakash. Mater. Chem. Phys., **307**, 128108 (2023). DOI: 10.1016/j.matchemphys.2023.128108

[5] N. Vela, M. Calín, M.J. Yáñez-Gascón, I. Garrido, G. Pérez-Lucas, J. Fenoll, S. Navarro. J. Photochem. Photobiol. A, **353**, 271–278 (2018). DOI: 10.1016/j.jphotochemrev.2017.11.040

[6] C.S. Turchi, D.F. Ollis. J. Catal., **122** (1), 178–192 (1990). DOI: 10.1016/0021-9517(90)90269-P

[7] Y. Nosaka, A.Y. Nosaka. Chem. Rev., **117** (17), 11302–11336 (2017). DOI: 10.1021/acs.chemrev.7b00161

[8] T. Wang, H. Liu, X. Wang, L. Tang, J. Zhou, X. Song, L. Lv, W. Chen, Y. Chen, X. Li. ACS Catal., **13** (21), 13902–13911 (2023). DOI: 10.1021/acscatal.3c01478

[9] C. Zhang, X. Wang, J. Du, Z. Gu, Y. Zhao. Adv. Sci., **8** (3), 2002797 (2021). DOI: 10.1002/advs.202002797

[10] Y. Li, W. Zhang, J. Niu, Y. Chen. ACS Nano, **6**, 5164–5173 (2012). DOI: 10.1021/nn300934k

[11] J. Ge, Y. Zhang, Y.-J. Heo, S.-J. Park. Catalysts., **9**, 122 (2019). DOI: 10.3390/catal9020122

[12] D. Bulyga., S.K. Evstropiev. Opt. Spectrosc., **130** (9), 1188–1196 (2022). DOI: 10.21883/eos.2022.09.54839.3617-22

[13] B.M. Namoos, A.R. Mohamed, K.A. Ali. J. Solid State Chem., **320**, 123834 (2023). DOI: 10.1016/j.jssc.2023.123834

[14] T. Wang, B. Tian, B. Han, D. Ma, M. Sun, A. Hanif, D. Xia, J. Shang. Energy & Environ. Mater., **5**, 711–730 (2022). DOI: 10.1002/eem2.12229

[15] Ranjbari, K. Demeestere, F. Verpoort, K.-H. Kim, P.M. Heynderick. Chem. Engin. J., **431** (4), 133349 (2022). DOI: 10.1016/j.cej.2021.133349

[16] F. Achouri, S. Corbel, L. Balan, K. Mozet, E. Girot, G. Medjahdi, M.B. Said, A. Ghrabi, R. Schneider. Mater. Design., **101**, 309–316 (2016). DOI: 10.1016/j.matdes.2016.04.015

[17] S. Lamkhao, S. Tandorn, G. Rujijanagul, C. Randorn. Mater. Today Sust., **23**, 100482 (2023). DOI: 10.1016/j.mtsust.2023.100482

[18] S.K. Evstropiev, A.V. Karavaeva, V.N. Vasilyev., N.V. Nikonorov, V.A. Aseev, K.V. Dukelskii, L.L. Lesnykh. J. Mater. Sci. Engin. B, **264**, 114877 (2021). DOI: 10.1016/j.mseb.2020.114877

[19] S. Das, V.C. Srivastava. Nanotechnol. Rev., **7** (3), 267–282 (2018). DOI: 10.1515/ntrev-2017-0144

[20] J. Aliaga, N. Cifuentes, G. González, C. Sotomayor-Torres, E. Benavente. Catalysts, **8**, 374 (2018). DOI: 10.3390/catal8090374

[21] H. Lachheb, F. Ajala, A. Hamrouni, A. Houas, F. Parino, L. Palmisano. Catal. Sci. Technol., **7**, 4041–4047 (2017). DOI: 10.1039/c7cy01085k

[22] A.A. Shelemanov, R.K. Nuryev, S.K. Evstropiev, V.M. Kiselev., N.V. Nikonorov. Opt. Spectrosc., **129** (12), 1300–1305 (2021). DOI: 10.1134/S0030400X21090198

[23] V. Etacheri, R. Roshant, V. Kumar. ACS Appl. Mater. Interfaces., **4** (5), 2717–2725 (2012). DOI: 10.1021/am300359h

[24] A. Hamrouni, N. Moussa, F. Parrino, A. Di Paola, A. Hous, L. Palmisano. J. Molec. Catal. A, **390**, 133–141 (2014). DOI: 10.1016/j.molcata.2014.03.018

[25] R. Ebrahimi, K. Hosseinsadeh, A. Maleki, R. Ghanbari, R. Rezaee, M. Safari, B. Shahmoradi, H. Daraei, A. Jafari, K. Yetilmezsoy, S.H. Puttaiah. J. Environ. Health Sci. Engin., **17**, 479–492 (2019). DOI: 10.1007/s40201-019-00366-x

[26] S. Evstropiev, A. Shelemanov, I. Bagrov, A. Karavaeva, K. Portnova, N. Nikonorov. Catal. Res., **4** (3) (2024). DOI: 10.21926/cr.2403008

[27] Vaishali Amrute, A. Monika, K.K. Supin, M. Vasundhara, Anupama Chanda. RSC Adv., **14**, 32786–32801 (2024). DOI: 10.1039/d4ra05197a

[28] M.V. Gallegos, M.A. Peluso, H. Thomas, L.C. Damonte, J. Sambeth. J. Alloys Comp., **689**, 416–424 (2016). DOI: 10.1016/j.jakkcom.2016.07.283

[29] Z. Gültekin, M. Alper, M.C. Hacıismailoğlu, C. Akay. J. Mater. Sci.: Mater. Electron., **34**, 438 (2023). DOI: 10.1007/s10854-023-09886-7

[30] K.V. Dukel'skii, S.K. Evstrop'ev. J. Optical Technology, **78** (2), 137–144 (2011). DOI: 10.1364/JOT.78.000137.
[31] T. Daimon, Y. Nosaka. J. Phys. Chem. C, **111**, 4420–4424 (2007). DOI: 10.1021/jp070028y
[32] M.B. Hillyer, J.H. Jourdan, S. Nam, M.W. Easson, B.D. Condon. Nanomater., **12**, 1621 (2022). DOI: 10.3390/nano12101621
[33] I.A. Pronin, B.V. Donkova, D.Tz. Dimitrov, I.A. Averin, J.A. Pencheva, V.A. Moshnikov. Semiconductors, **48** (7) 842–847 (2014). DOI: 10.1134/s1063782614070173.
[34] Z. Zainal, L.K. Hui, M.Z. Hussein, Y.H. Taufiq-Yap, A.H. Abdullah, I. Ramli. J. Hazard. Mater., **125**, 113–120 (2005). DOI: 10.1016/j.jhazmat.2005.05.013
[35] H. Morkoç, Ü. Özgür. *Zinc Oxide: Fundamentals, Materials, and Device Technology* (Wiley-VCH, Berlin, 2009). DOI: 10.1002/9783527623945
[36] R.D. Shannon. Acta Cryst., **32**, 751–767 (1976). DOI: 10.1107/s0567739476001551
[37] Z. Ma, F. Ren, X. Ming, Y. Long, A.A. Volinsky. Materials, **12** (1), 196 (2019). DOI: 10.3390/ma12010196
[38] O. Bilgili. Acta Phys. Polonica A, **136** (3), 460–466 (2019). DOI: 10.12693/APhysPolA.136.460
[39] C.-Y. Tsay, M.-C. Wang, S.-C. Chiang. Mater. Trans., **49** (5), 1186–1191 (2008). DOI: 10.2320/matertrans.MER2007334
[40] L. Srinivasa Rao, T. Venkatappa Rao, Sd. Naheed, P. Venkateswara Rao. Mater. Chem. Phys., **203**, 133–140 (2018). DOI: 10.1016/j.matchemphys.2017.09.048
[41] E.H. Kisi, M.M. Elcombe. Acta Cryst. Struct. Commun., **45** (12), 1867–1870 (1989). DOI: 10.1107/S0108270189004269
[42] R. Ullah, J. Dutta. J. Hazard. Mater., **156** (1−3), 194–200 (2008). DOI: 10.1016/j.jhazmat.2007.12.033
[43] S. Lagergren. Handlingar, **24**, 1–39 (1898).
[44] C. Tian, H. Zhao, H. Sun, K. Xiao, P.K. Wong. Chem. Engin. J., **381**, 122760 (2020). DOI: 10.1016/j.cej.2019.122760
[45] E.D. Revellame, D.L. Fortela, W. Sharp, R. Hernandez, M.E. Zappi. Clean. Engin. Technol., **1**, 100032 (2020). DOI: 10.1016/j.clet.2020.100032
[46] S. Phromma, T. Wutikhun, P. Kasamechonchung, T. Eksangsri, C. Sapcharoenkun. Appl. Sci., **10**, 993 (2020). DOI: 10.3390/app10030993

Translated by A.Akhtyamov